Effect of strain-induced crystallization on fatigue crack growth resistance of natural rubber

Pierre Rublon, Bertrand Huneau, Erwan Verron, Nicolas Saintier, Daniel Berghezan

Effect of crystallization on fatigue crack growth resistance of natural rubber

P. Rublon & B. Huneau & E. Verron
LUNAM Université, Ecole Centrale de Nantes, GeM-UMR CNRS 6183, Nantes, France

N. Saintier
I2M-DuMAS, UMR 5295 CNRS, Arts et Métiers ParisTech, Talence, France

D. Berghezan
Manufacture Française des Pneumatiques Michelin, Centre Technique de Ladoux, Clermont-Ferrand, France

ABSTRACT: In tire industry, fatigue crack propagation in elastomers is usually investigated to improve the service life of products. To explain the remarkable resistance to fatigue crack growth in natural rubber as compared to synthetic rubbers, the literature often mentions the strain-induced crystallization (SIC) phenomenon that takes place at the tip of fatigue cracks in such a material. This study presents an original experimental set-up that couples synchrotron radiation with a homemade fatigue machine and permits the real time investigation of the crystallized zone at crack tip during uninterrupted fatigue tests. Diffraction patterns' recording is synchronized with the cyclic loading to perform a "mapping" of wide-angle X-ray diffraction (WAXD) measurements, in order to obtain the 2D spatial distribution of crystallinity in the neighbourhood of the crack tip. The influence of different parameters, such as the loading conditions (level of cyclic stretching) or the carbon-black filler content, on the size of the crystallized zone, is investigated. The comparison of these results with fatigue crack propagation tests performed with the same experimental conditions and the same materials leads to a first explanation of the very good macroscopic fatigue behaviour in natural rubber samples.

1 INTRODUCTION

The impressive resistance of natural rubber (NR) to fatigue crack growth as compared to others synthetic rubbers, has been reported by many authors in the literature (Lake and Lindley 1965, Lake 1995, Mars and Fatemi 2004, among others). The srain-induced crystallization (SIC) phenomenon, that takes place in particular in the neighbourhood of a crack tip (Trabelsi et al. 2002, Lee and Donovan 1987) because of large strains in this region, is believed to play a major role and would slow down the crack advance during a fatigue test (Mars and Fatemi 2003, Mars and Fatemi 2004, Saintier et al. 2010). However, the influence of the crystallized zone at the crack tip on the crack propagation in fatigue remains unproven today.

In this context, the present paper aims to relate the measurements of fatigue crack propagation rates in NR samples with the characteristics of the crystallized zone around the crack tip in order to explain this good macroscopic behaviour. To do this, two experimental methods and their results are compared:

- On the one hand, classical fatigue crack propagation tests are performed on different pre-cracked "Pure Shear" samples of NR filled with various amounts of carbon black, to evaluate the crack propation rate.

- On the other hand, in-situ fatigue tests are conducted with almost the same loading conditions at the French national synchrotron facility SOLEIL, to measure in real time the crystallinity in the vicinity of the crack tip by mapping this region with Wide-Angle X-ray Diffraction (WAXD) measurements. This original experimental method, described in details in Rublon et al. (2013), permits to determine the SIC distribution around the crack during uninterrupted fatigue tests.

After the description of the experimental set-up and methods, the end of the paper discusses the different results, in order to solve the question of the influence of SIC on the fatigue crack growth behaviour of natural rubber.

2 EXPERIMENTAL METHOD

2.1 *Materials and samples*

Four elastomers with the same gum of NR but with various amounts of N347 carbon black (CB N347) are used (0, 30, 50 and 70 phr) in order to evaluate the influence of fillers. Vulcanization is carried out with 1.6 phr of sulphur, where CBS acts as an accelerator. Each blend also contains ZnO and stearic axid. 6PPD is used as an antioxydant. As a comparison, a synthetic isoprene rubber (IR) filled with 50 phr of CB N347 and with exactly the same amounts of additives NR compounds, is also used. In IR, the SIC is considerably reduced compared to NR, and the results obtained on this material are very helpful to discuss the influence of this phenomenon. The respective formulation of those five materials are given in Table 1. The geometry of the samples is a classical "Pure Shear" geometry (PS), commonly employed for fatigue crack growth tests in the literature (Young 1985, Andreini et al. 2013), whose dimensions are 157 mm long, 13 mm high and 2 mm thick.

Table 1: Materials formulation

	NR0	NR30	NR50	NR70	IR50
Ingredients	Content (phr)				
NR	100	100	100	100	-
IR	-	-	-	-	100
Carbon black N347	0	30	50	70	50
Stearic acid	2	2	2	2	2
Zinc oxyde	2.5	2.5	2.5	2.5	2.5
CBS accelerator	1.6	1.6	1.6	1.6	1.6
6PPD	1.9	1.9	1.9	1.9	1.9
Sulphur	1.6	1.6	1.6	1.6	1.6

2.2 *Fatigue crack growth rate tests*

Fatigue crack propagation measurements are based on the energy balance approach of Rivlin and Thomas (Rivlin and Thomas 1953), who have extended the initial theory of energy release rate formulated by Griffith in his seminal paper (Griffith 1921). Considering thin samples of uniform thickness h_0 and denoting c the crack length, they defined the "tearing energy" T by:

$$T = -\frac{1}{h_0}\frac{\partial w}{\partial c}\bigg|_l \tag{1}$$

where w is the strain energy and the suffix $._l$ denotes differentiation with constant displacement of the boundaries over which forces are applied. In the case of PS samples, they demonstrated the following relation between T, W_0 the strain energy density and l_0 the height of the undeformed sample:

$$T = W_0 l_0 \tag{2}$$

All the tests were performed at Michelin (Clermont-Ferrand, France) on a MTS servo-hydrolic fatigue machine. After clamping, the sample is first cycled during 300 cycles at a global stretch ratio ($\lambda = l/l_0$) of 1.92 at 2Hz, to supress the Mullins effect and lower the residual stretch due to an inherent viscous behaviour. Cyclic tests with uncracked samples are then conducted at different stretch ratios from 1.08 to 1.92 in order to determine the strain energy density W_0 as a function of the global stretch ratio, by integration of the area under the stress-strain curve. After the insertion of three notches (which entails 4 crack tips) in the sample at the edges (2cm-long) and in the middle of the test piece (3cm-long), a short preliminary cyclic test is performed to blunt the crack tips and to transform cutter incisions into fatigue cracks. After all, the procedure of fatigue crack growth experiments is applied, by cycling the cracked sample at a frequency of 2Hz and for different global stretch ratios (corresponding to different values of T). The cyclic tests are paused several times to measure the mean value of the advance of the 4 cracks with a binocular microscope, from which is deduced the crack growth rate (dc/dn in nm/cycle). A conventional way to represent the results is a log-log (dc/dn) vs. T plot (Lake 1995).

2.3 *In-situ synchrotron WAXD experiments*

The in-situ WAXD measurements are conducted with a homemade fatigue machine using two electrical actuators which supply a cyclic sinusoidal displacement to the rubber sample. This machine is fixed on a mobile diffractometer on the DiffAbs beamline at the French national synchrotron facility SOLEIL. The wavelength of the beam is 0.1305 nm and the beam-size is approximately 300 μm x 200 μm (full width at half maximum height). The two-dimensional WAXD patterns are recorded by a MAR CCD X-ray detector (SX-165) with an exposure time of $1s$. The transmitted beam is blocked by a Pb beamstop on which a Si PIN photodiode is placed to measure the transmitted intensity through the rubber and thus, estimate the thickness of the sample. After almost the same sample preparation as the one described in the previous section 2.2, except the fact that only one notch is introduced at the edge of the sample, the procedure of WAXD acquisition starts. It consists in a mapping of the neigbourhood of the crack tip with 90 WAXD measurements without stopping cyclic loading, by acquiring diffraction data at the top of each cycle and moving the sample with respect to the beam between two cycles in order to perform the next WAXD acquisition on an other point of the map. Figure 1 summarizes this procedure, which is fully described in Rublon et al. (2013).

However, the determination of the index of crystallization is here quite different from the procedure described in Rublon et al. (2013), in order to take into account this time, the oriented amorphous phase and the influence of carbon black fillers. It consists in ex-

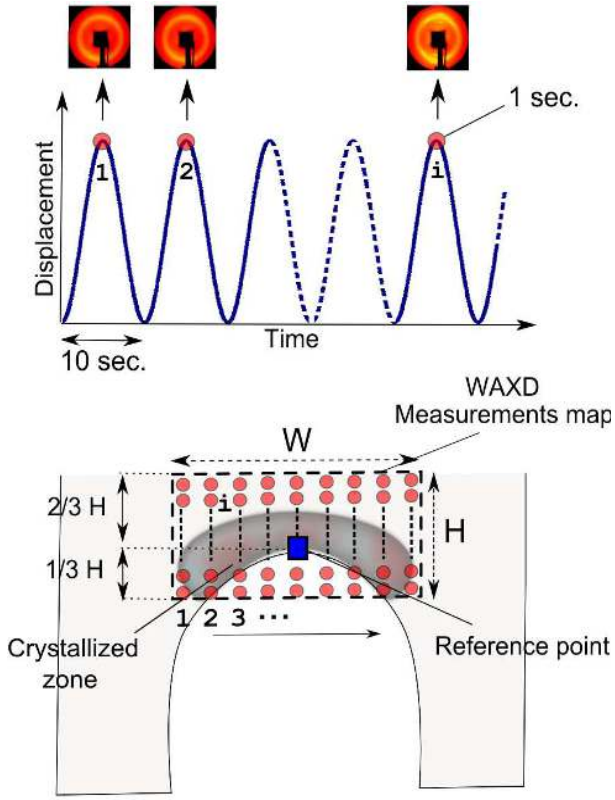

Figure 1: WAXD measurements during fatigue tests. Top: each diffraction pattern is recorded at the maximum displacement of each cycle. Bottom: between two measurements, the sample moves with respect to the beam to reach the next point on the prescribed map.

tracting the total diffracted intensity (averaged over an azimuthal angle of 45 °), at the azimuthal angle corresponding to the (200) and the (120) Bragg reflections, from which we can deconvolute with Pearson VII functions, different amorphous and crystallized peaks and an other peak due to the addition of CB. The deconvolution of a typical pattern is given in Figure 2. An index of crystallinity is then defined by:

$$\chi = \frac{\int I_{200}}{\int I_{200} + \int I_{amorphous}} \tag{3}$$

where $\int I_{200}$ is the integrated area of the (200) peak and $\int I_{amorphous}$ the integrated area of the amorphous

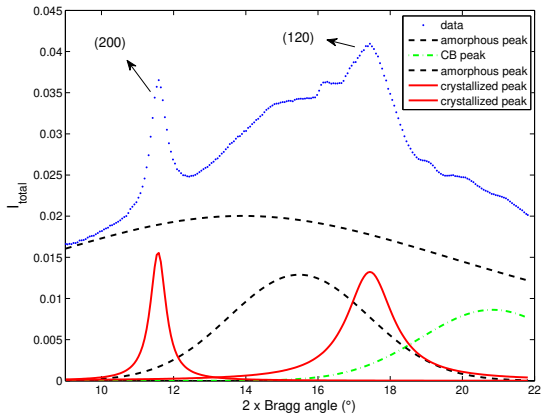

Figure 2: Deconvolution and fitting of a pattern.

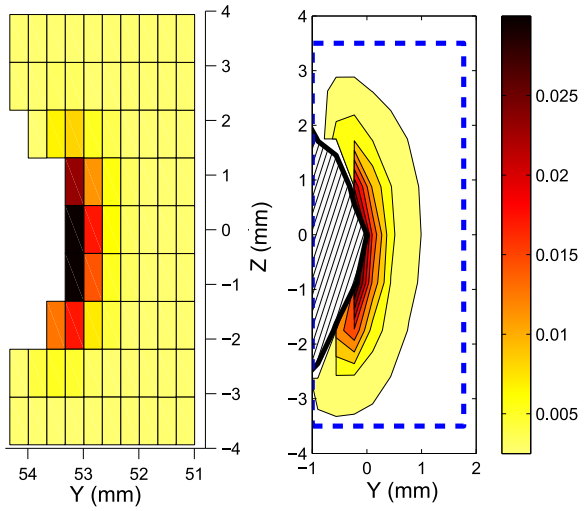

Figure 3: Raw data (left) and post-processed data (right) of the index of crystallinity χ at a fatigue crack tip in a NR filled with 50 phr of CB N347, at a global stretch ratio of $\lambda = 1.92$ and a corresponding tearing energy of $T = 14140 J/m^2$. The hatched area represents the crack and dotted line show the limits of the measurement map.

peaks. It is to note that, in order to consider the orientation of the amorphous phase during elongation of the sample, the amorphous intensity is averaged in the polar and equatorial directions.

Those measurements lead finally to the plot of iso-χ curves around the identified crack tip, as depicted in figure 3. Moreover, taking into account the value of the transmitted intensity as a measurement of the thickness, it is also possible to evaluate the volume around the crack tip in which the SIC phenomenon occurs.

3 RESULTS AND DISCUSSION

3.1 *Fatigue crack growth tests*

3.1.1 *NR50 vs. IR50*

The fatigue crack growth behaviour of a NR filled with 50 phr of CB (NR50) is first compared to the behaviour of an IR filled with the same amount of fillers (IR50). The results are presented in Figure 4. First of all, we notice that for a given tearing energy T, the crack growth rate is lower in the case of NR50, and this is especially true for high values of T. This is consistent with the different results of the literature, in particular those of Lake (1995), who found a similar behaviour between a filled NR and a filled SBR.

3.1.2 *Influence of carbon black fillers*

The influence of CB N347 fillers on fatigue crack growth behaviour is reported in Figure 5. It appears that the resistance to crack advance is improved with the addition of fillers, if we compare the unfilled natural rubber (NR0) with the filled ones. Moreover, the slope of the curve seems to be lower in the case of filled NR. Those results tend to confirm the results already obtained by Papadopoulos et al. (2008), who

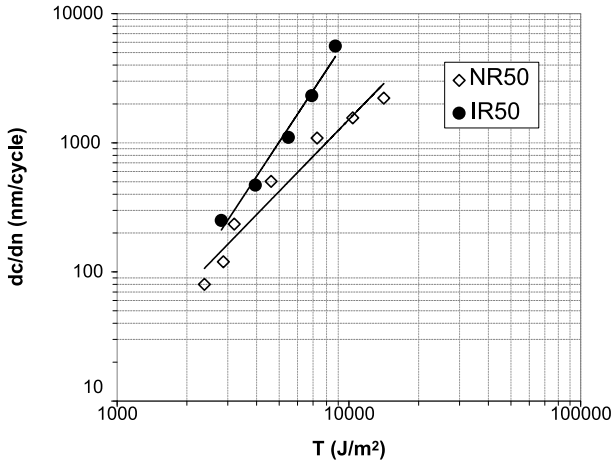

Figure 4: Fatigue crack growth rate behaviour of a NR50 sample (unfilled symbols) and a IR50 sample (filled symbols). With the doubly logarithmic plot, the black straight lines represent simple power law relationship (slopes of the curves: 1.70 for NR50, 2.73 for IR50)

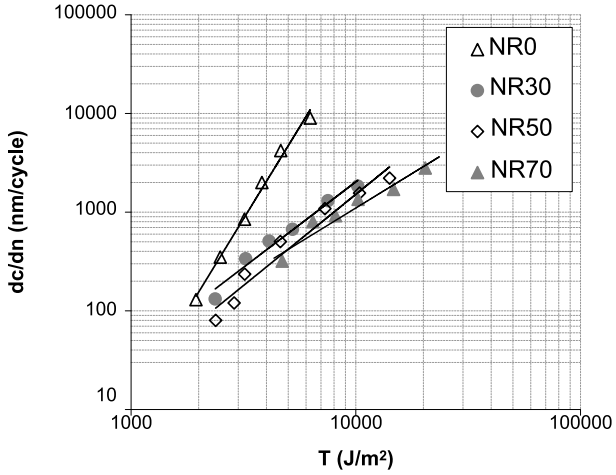

Figure 5: Fatigue crack growth rate measured on NR0, NR30, NR50 and NR70 samples. With the doubly logarithmic plot, the black straight lines represent simple power law relationship (slopes of the curves: 3.72 for NR0, 1.73 for NR30, 1.85 for NR50 and 1.34 for NR70)

compared the fatigue crack growth resistance of a 23 phr CB filled NR with an unfilled one. However, if one looks only at the filled rubbers, the CB content does not seem to impact significantly the crack growth behaviour and just a small decrease of dc/dn is observed when increasing the amount of fillers.

3.2 *WAXD experiments results*

3.2.1 *NR50 vs. IR50*

Figure 6 presents the iso-crystallinity curves obtained after the WAXD measurements performed around a fatigue crack tip of NR50 for four differents values of tearing energy T. It emphasizes the noteworthy influence of this parameter on the size of the crystallized zone. The values of the transmitted intensity at each point of the map permit to quantify this result with the evaluation of the volume where crystallites are detected in the neighbourhood of the crack tip, as reported in figure 7 for the four previous values of T. As SIC phenomenon is almost null for IR50 sample, the values of the crysallized volume are put equal to zero in this graph.

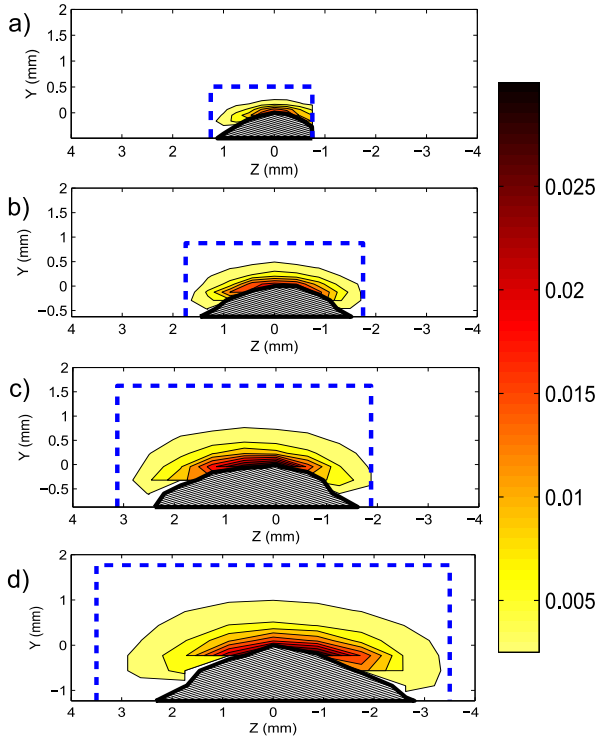

Figure 6: Distribution of the index of crystallinity around a fatigue crack tip in NR50 for 4 different values of tearing energy: a) $T = 4620 J/m^2$ b) $T = 7290 J/m^2$ c) $T = 10390 J/m^2$ d) $T = 14140 J/m^2$. The lowest value of the index, corresponding to the limit of detected crystallisation, is 0.002.

3.2.2 *Influence of carbon black fillers*

The influence of CB content on the size of the crystallized zone at crack tip was also investigated. Figure 8 provides the crystallized volume obtained on four different NR filled with various amounts of fillers, as a function of tearing energy T. One notes that the expected effect of fillers is quite hard to notice and on the contrary, it appears that, whatever the CB content, a given tearing energy T leads to a same value of crystallized volume at fatigue crack tip, revealing a master curve in Figure 8.

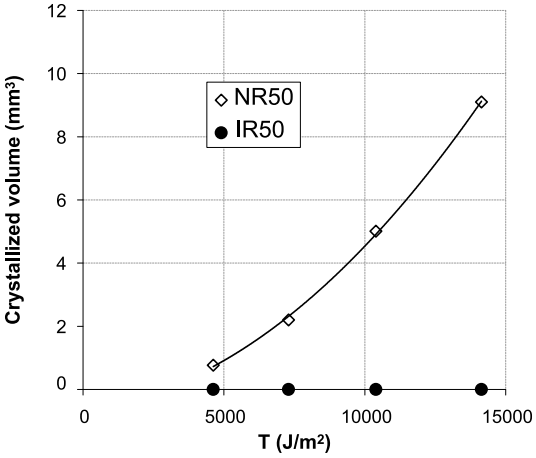

Figure 7: Volume where crystallinity is detected as a function of tearing energy for NR50 and IR50. The line represents a power law relationship fitted on the values relative to the NR50 sample.

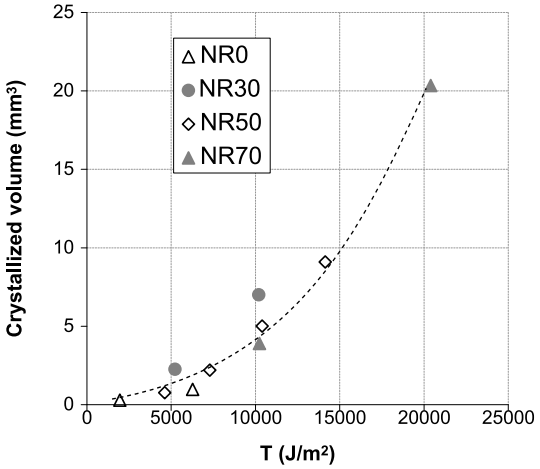

Figure 8: Volume where crystallinity is detected as a function of tearing energy for four NR compounds filled with various amounts of CB. The dotted line just gives the tendency of the data.

3.3 *Discussion*

- First, the results of crack growth measurements shown in Figure 4 and the evolution of the crystallized volume at crack tip with tearing energy plotted in Figure 7 can be related. On the one hand, the resistance to fatigue crack growth in NR is greater than the one in IR, and even more for high values of T. On the other hand, the volume of the crystallized zone at crack tip increases with T. Recalling that SIC is considerably lower in IR, it proves that crystallization at crack tip slows down the crack advance. To sum up this idea: the higher the tearing energy, the larger the crystallized zone at crack tip and the lower the crack growth rate.

- Second, one cannot propose the same kind of conclusion by comparing NR samples with different amounts of CB. Indeed, the differences observed on the crack growth behaviour of the materials in Figure 5 are not explained by the crystallized volume measured at crack tip on the same materials, taking into account the master curve appearing in Figure 8. It is consistent with the fact that the improvement of the resistance to fatigue crack growth with CB fillers is also reported on rubbers which do not crystallize at all (Papadopoulos et al. 2008).

- Finally, the tearing energy appears to be a parameter of most importance in the phenomenon of SIC at a fatigue crack tip in NR, and may govern it whatever the carbon black content.

4 CONCLUSION

An original experimental set-up consisting in the association of a homemade fatigue machine with synchrotron radiation, allows the measurement of the crystallized zone at crack tip of NR during fatigue tests. The comparison of those results with fatigue crack growth rates measurements with almost the same conditions of cyclic stretching permits to understand the effect of SIC on fatigue crack propagation of NR and gives a first explanation of the well-known resistance to fatigue crack growth of NR. Furthermore, the comparison of different samples of NR with various amounts of CB fillers underlines the importance of the tearing energy parameter on the size of the crystallized zone in the crack tip neigbourhood.

AKNOWLEDGMENT

The authors thank Dr. Dominique Thiaudiere and Dr. Cristian Mocuta for their great help on this project. All the reported diffraction measurements were performed on DiffAbs beamline at synchrotron SOLEIL, Gif-sur-Yvette, France (proposal 20110204).

REFERENCES

Andreini, G., P. Straffi, S. Cotugno, G. Gallone, & G. Polacco (2013). Crack growth behavior of styrene-butadiene rubber, natural rubber, and polybutadiene rubber compounds: comparison of pure-shear versus strip tensile test. *Rubber chemistry and technology* (DOI:), 10.5254/rct.13.88957.

Griffith, A. (1921). The phenomena of rupture and flow in solids. *Philosophical Transactions of the Royal Society of London A 221*, 163–198.

Lake, G. (1995). Fatigue and fracture of elastomers. *Rubber chemistry and technology 68*(3), 435–460.

Lake, G. & P. Lindley (1965). Mechanical fatigue limit for rubber. *Journal of applied polymer science 9*(4), 1233–1251.

Lee, D. & J. Donovan (1987). Microstructural changes in the crack tip region of carbon-black-filled natural rubber. *Rubber chemistry and technology 60*, 910–923.

Mars, W. V. & A. Fatemi (2003). A phenomenological model for the effet of R ratio on fatigue of strain crystallizing rubbers. *Rubber chemistry and technology 76*(5), 1241–1258.

Mars, W. V. & A. Fatemi (2004). Factors that affect the fatigue life of rubber: a literature survey. *Rubber chemistry and technology 77*(3), 391–412.

Papadopoulos, I. C., A. G. Thomas, & J. J. C. Busfield (2008). Rate Transitions in the Fatigue Crack Growth of Elastomers. *Journal of applied polymer science 109*(3), 1900–1910.

Rivlin, R. & A. Thomas (1953). Rupture of rubber. *Journal of polymer science 10*(3), 291–318.

Rublon, P., B. Huneau, N. Saintier, S. Beurrot, A. Leygue, E. Verron, C. Mocuta, D. Thiaudière, & D. Berghezan (2013, January). In situ synchrotron wide-angle X-ray diffraction investigation of fatigue cracks in natural rubber. *Journal of synchrotron radiation 20*, 105–109.

Saintier, N., G. Cailletaud, & R. Piques (2010, October). Cyclic loadings and crystallization of natural rubber: An explanation of fatigue crack propagation reinforcement under a positive loading ratio. *Materials Science and Engineering: A 528*(3), 1078–1086.

Trabelsi, S., P.-A. Albouy, & J. Rault (2002, December). Stress-Induced Crystallization around a Crack Tip in Natural Rubber. *Macromolecules 35*(27), 10054–10061.

Young, D. (1985). Dynamic property and fatigue crack propagation research on tire sidewall and model compounds. *Rubber chemistry and technology 58*(4), 785–805.